The Differential Degradation of Two Cytosolic Proteins As a Tool to Monitor Autophagy in Hepatocytes by Immunocytochemistry

Catherine Rabouille,* Ger J. Strous,* James D. Crapo,‡ Hans J. Geuze,* and Jan W. Slot*

*Department for Cell Biology, Utrecht University School of Medicine, 3584 CX, Utrecht, The Netherlands; and
‡Pulmonary Division, Duke University Medical Center, Durham, North Carolina 27710

Abstract. The major pathway for cytosolic constituents to enter lysosomes is by autophagy. We used two cytosolic proteins, CuZn superoxide dismutase (SOD) and carbonic anhydrase III (CAIII), as autophagic markers in male rat hepatocytes. We took advantage of the differential presence of the two proteins in autophagic vacuoles because of the high resistance of SOD to lysosomal degradation as compared with CAIII. This allows us to determine the sequence of autophagic vacuole formation. We have double immunogold-labeled SOD and CAIII in cryosections of fasted rat liver and calculated the ratios of SOD over CAIII labeling densities (SOD/CAIII) in autophagic vacuoles (AV), as compared with the cytoplasm. Different classes of AV were defined according to their SOD/CAIII, their morphology, and their additional immunolabeling for the lysosomal markers lgp120 and cathepsin D. Of all AV, 15% exhibited a cytosol-like SOD/CAIII, indicating that degradation had not yet begun. Most of these initial AV (AVi) showed two enveloping membranes. The formation of AVi was prevented by 3-methyladenine, a potent inhibitor of autophagy. Of all AV, 85% showed a SOD/CAIII that exceeded the cytosolic ratio. These single membrane-bound vacuoles were called degradative AV (AVd). Labeling for lysosomal markers allowed the characterization of AV that shared features with both AVi and AVd. These AVi/d had a cytosol-like SOD/CAIII and a double membrane, but showed some labeling for lysosomal markers. Probably these AVi/d represent the recipient compartment for lysosomal components. AVd were positive for cathepsin D and lgp120. We discerned two AVd subclasses. Early AVd with cytosol-like SOD labeling density while CAIII labeling density was consistently lower than in the cytosol. Their size was similar to AVi and AVi/d. Late AVd contained higher SOD concentrations and were mostly larger. Our findings suggest that AV acquire lysosomal constituents by fusion with small nonautophagic structures and that after subsequent elimination of the inner membrane of AVi, degradation starts resulting in the formation of early AVd and late AVd.

MATERIALS are transported to lysosomes via four pathways: (1) the biosynthetic pathway for delivery of newly synthesized hydrolases and other constitutive compounds; (2) the endocytotic and phagocytotic pathways for uptake of extracellular constituents; (3) the specific targeting of cytosolic proteins such as described for proteins carrying KFERQ-related sequences (Chiang and Dice, 1986); and (4) the autophagic route by which cells degrade parts of their own content.

Although substantial knowledge has been collected about pathways 1, 2, and 3 (for reviews, see Kornfeld and Mellman, 1989; Gruenberg and Howell, 1989; Chiang et al., 1989), the autophagic route has been difficult to approach experimentally. One way is to use intracellularly administered compounds like sucrose and lactose (Seglen, 1987; Gordon and Seglen, 1988); however, such low molecular weight markers are not suitable for morphological observations. Contributions to the field using electron microscopy are largely restricted to descriptive studies of autophagic vacuoles at various stages of degradative activity (Marzella and Glaumann, 1987). One exception is the study of Tooze et al. (1990), who followed sequential steps in autophagy after inducing artificial protein complexes in the ER. However, their observations were restricted to the degradation of these complexes while, in general, autophagy is thought to be a nonspecific process in which cytoplasmic proteins are degraded randomly. This has recently been illustrated by Kopitz et al. (1990), who found similar rates for autophagic degradation of seven cytosolic proteins of the rat liver.

The autophagic process is very well developed and regulated in rat liver parenchymal cells, where it can be induced by fasting the animal (Mortimore, 1987), addition of glucagon (Schworer and Mortimore, 1979), or removal of amino acids from the incubation medium of isolated hepatocytes (Seglen and Bohley, 1992). Fasting was recently used by Dunn (1990*a*, *b*) to synchronize autophagy in a liver perfusion system, so that the sequential steps of the autophagic process could be monitored morphologically. Autophagy

starts with the formation of the initial autophagic vacuoles (AVi)[1] in which portions of cytoplasm are randomly sequestered by a membrane which is thought to develop from rough ER (Dunn, 1990*a*; Furuno, 1990). AVi lack lytic capacities. Maturation of the AVi involves the acquisition of lytic enzymes, resulting in a degradative autophagic vacuole (AVd). Dunn's studies contributed significantly to the characterization of the different autophagic compartments and their relationship to other cell structures by use of an extensive set of molecular markers in immuno- and enzyme-cytochemistry. However, the lack of typical autophagic markers analogous to markers used in studies on endocytosis rendered a direct tracing of the degradation itself impossible. Thus, it remains to be defined where degradation actually starts and where the autophagic route meets other degradative pathways.

In the present study, we describe that the two common cytosolic proteins in rat liver cells, the copper-zinc containing superoxide dismutase (SOD) and the type III isoenzyme of carbonic anhydrase (CAIII), have greatly different proteolytic resistances. We use this difference to monitor the developmental stages of autophagy in rat liver by immunogold cytochemistry. Previous studies (Slot et al., 1986; Chang et al., 1988; Laurila et al., 1989) have shown that both proteins are localized in the cytosol. Based on the observation that SOD but not CAIII is present in lysosomes, our working hypothesis is that after random autophagic sequestration of cytosol, SOD accumulates in lysosomes because of its proteolytic resistance while CAIII disappears during maturation of AVi into AVd by lysosomal degradation. Using semiquantitative immunocytochemistry and cell fractionation after autophagy stimulating and inhibiting conditions, we collected new data on the sequence of autophagic events in rat liver cells such as the introduction of lytic enzymes, fusion of vacuoles, and changes in the concentration of content.

Materials and Methods

In Vitro Degradation of SOD and CAIII

Male Wistar rats weighing 200 g were fasted for 24 h. After anesthesia by intraperitoneal injection of pentobarbital, the liver was excised and put in ice cold 0.25 M sucrose in 0.2 M KCl. Crude lysosomal fractions were prepared according to De Duve et al. (1955). After homogenizing twice in a loose fitting Potter and centrifugation at 650 *g* for 5 min, the supernatant was collected and centrifuged at 12,000 *g* for 30 min. The resulting pellet (p2) contained lysosomal vacuoles, mitochondria, and peroxisomes (De Duve et al., 1955). The supernatant (sup2) was kept and used as a source of cytosolic proteins. The p2 was washed three times with 0.25 M sucrose in 0.2 M KCl by successive centrifugation at 12,000 *g* for 30 min, resuspended in 2 ml of 0.25 M sucrose, 0.2 M KCl. 40-μl aliquots were first preincubated for 15 min at 37°C in 0.05 M sodium acetate, pH 4.5, supplemented with 0.1% Triton X-100. Then 100 μl of sup2 was added and the mixture incubated for various times (0–240 min). The reaction was stopped by adding 100 μl of SDS sample buffer and boiling for 5 min at 100°C. Control incubations (60 min) were performed by inhibiting proteases using 0.05 M Hepes, pH 8, instead of sodium acetate or leupeptin (0.05 mg/ml).

Samples were then analyzed by PAGE under reducing conditions according to the method of Laemmli (1970). The proteins were electrophoretically transferred to nitrocellulose (1 h, 0.8 mA/cm^2 on a semidry blotting apparatus [LKB Instruments, Inc., Bromma, Sweden]), and SOD and CAIII were detected by incubating the blot with both anti-SOD antisera (diluted 1:1,000) (Chang et al., 1988) and anti-CAIII antisera (diluted 1:500) (Laurila et al., 1989) followed by ^{125}I-protein A (1 mCi/200 mg, 1:10,000) and autoradiography as described by Rijnboutt et al. (1991). The intensity of the SOD and CAIII bands on the film was measured using a laser densitometer (Pharmacia LKB Technology Inc., Piscataway, NJ). Protein concentrations were measured according to the Bradford method (Bradford, 1976) with albumin as a standard.

Cell Fractionation of Isolated Hepatocytes

Fed male Wistar rats (200 g) were anesthetized and the liver was perfused with collagenase through the portal vein according to Beynen et al. (1979). The hepatocytes (wet weight 7.5 g total) were recovered and diluted 10 times in Krebs-Ringer containing 1 nM glucagon (Novo Biolab, Cambridge, UK) and 5 mM 3-methyladenine (3-MA; Fluka Chemie AG, Buchs, Switzerland) (Seglen and Gordon, 1982) and incubated for 30 min at 37°C. This was performed to stimulate glycogen degradation (glucagon) without inducing autophagy (3-MA). The cells were washed two times with Krebs-Ringer made up to the same volume, and aliquoted in 2-ml fractions in 20 ml erlenmeyers. Each sample contained about 20 million cells (Beynen and Geelen, 1984), and was supplemented by 1 nM glucagon to stimulate both the glycogen catabolism and the autophagic process (control incubation for autophagy). The incubation was performed at 37°C for 60 min. When indicated, the samples were supplemented during the incubation for autophagy with 10 mM 3-MA for the time of the incubation. Cells were recovered, washed, and resuspended in 1 ml of ice cold sucrose/Hepes/EDTA (0.25 M/10 mM/2 mM). The postnuclear supernatant (PNS) (800 *g* × 10 min) was recovered and kept on ice. One aliquot was taken for electrophoretic analysis. The PNS was incubated in the presence of amylase (0.2 mg/ml, Sigma Chem. Co., St. Louis, MO) for 1 h on ice and in the presence of proteinase K (0.2 mg/ml; Boehringer Mannheim Corp., Federal Republic of Germany) for 1 h on ice, and were layered on the top of 3 ml sucrose/Hepes/EDTA/PMSF (0.5 M/10 mM/2 mM/1 mM) and a cushion of 0.3 ml of 2 M sucrose in the same buffer in an ultracentrifuge polyallomer tube (No. 326819; Beckman Instrs., Inc., Fullerton, CA). The centrifugation was performed in an SW50 Beckman rotor at 100,000 *g* for 1 h at 4°C. The 1-ml bottom contained the membrane fraction in 0.95 M sucrose/10 mM Hepes/2 mM EDTA/1 mM PMSF (0.3 ml of 2 M sucrose + 0.7 ml of 0.5 M sucrose). Aliquots of the membrane fraction were taken and diluted twice in SDS sample buffer for SDS gel electrophoresis (13%) under reducing conditions as described above. After blotting (60 min, 35 V, 1.5 A in a Mini-Genie Electroblotter, Idea Scientific Co., Minneapolis, MN), the two bands corresponding to SOD and CAIII were fluorographed and scanned.

Electron Microscopy

Livers of fasted Wistar male rats were fixed by perfusion through the portal vein with a mixture of 2% paraformaldehyde and 0.2% glutaraldehyde in 0.1 M sodium phosphate buffer (pH 7.4) for 5 min after flushing the blood with PBS for 30 s. The liver was postfixed in the same mixture for 3 h. Hepatocytes were fixed in 2% glutaraldehyde for 1 h and embedded in 10% gelatin (Peters et al., 1991). Sometimes cells were broken mechanically and incubated 1 h on ice in the presence of proteinase K (0.2 mg/ml) before fixation. Small blocks of tissue and gelatin-embedded cells were prepared and infused with 2.3 M sucrose, placed on specimen holders, and frozen in liquid nitrogen. Ultrathin cryosections were cut with a Cryonova (Reichert/LKB, Vienna, Austria). The sections were immunolabeled as previously described (Slot et al., 1988). Briefly, they were incubated for 30 min with antibodies against CAIII (Laurila et al., 1989) or SOD (Slot et al., 1986; Chang et al., 1988) followed by marking with 10-nm protein A-gold. CAIII-SOD double labeling was performed by the sequential protein A method (Geuze et al., 1981) as modified recently (Slot et al., 1991). Sections were first labeled for CAIII with 15-nm protein A-gold. This immunoreaction was stabilized with 0.5% glutaraldehyde for 5 min before the section was incubated for SOD labeling with 10-nm protein A-gold. Triple-labeled sections first underwent the CAIII-SOD double labeling except that CAIII was visualized with 10-nm protein A-gold and SOD with 5-nm protein A-gold, and then again stabilized by glutaraldehyde and followed by incubation with a third antibody which was directed against a marker protein of the (pre)lysosomal compartment and 15-nm protein A-gold. For the third marking reaction, anti-lgp120 antibody (Geuze et al., 1988) or anti-cathepsin D antibody (Geuze et al., 1985) were used. After immunolabeling, ultrathin cryosections were stained with uranyl acetate and embedded in methyl cellulose according to Tokuyasu (1980).

1. *Abbreviations used in this paper*: AVd, degradative autophagic vacuoles; AVi, initial autophagic vacuoles; CAIII, carbonic anhydrase III; LD, labeling density; 3-MA, 3-methyladenine; PNS, postnuclear supernatant; SOD, copper zinc superoxide dismutase.

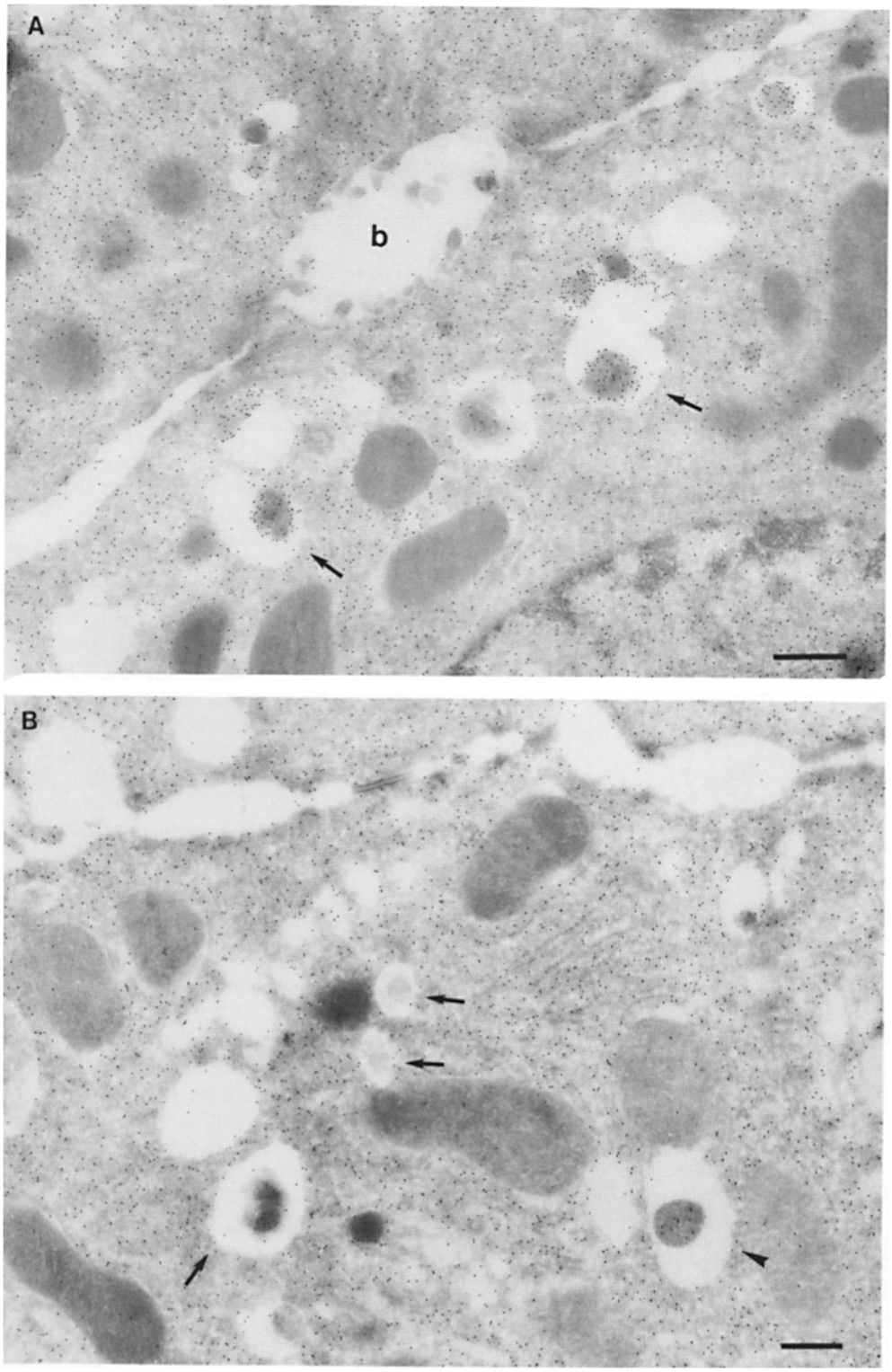

Figure 1. Localization of SOD and CAIII in parenchymal rat liver cells. Cryosections from male fasted rat liver were immunolabeled for (*A*) SOD and (*B*) CAIII with 10-nm gold. The cytoplasm adjacent to the bile caniculus (*b*) contains many lysosome-like structures which are heavily labeled for SOD (*arrows* in *A*) but hardly for CAIII (*arrows* in *B*) except for a minority of vacuoles in which CAIII labeling is approximatively the same as in the cytoplasm (*arrowhead* in *B*). Bars, 500 nm.

Quantitation

For autophagic vacuoles SOD/CAIII was calculated by dividing the number of SOD gold particles by the number of CAIII gold particles. For the cytoplasm, the same calculation has been performed by analyzing random areas of μm^2.

To calculate the concentration factor for SOD in an autophagic vacuole, the number of gold particles per μm^2 in its profile was taken as the labeling density of SOD (LD-SOD) for that vacuole. Similarly we established the LD-SOD in the surrounding cytoplasm. The concentration factor for SOD is then: $LD\text{-}SOD_{autophagic\ vacuole}/LD\text{-}SOD_{cytoplasm}$.

To estimate the surface area of autophagic vacuoles in the sections, we used the average of the longest and shortest axes of the vacuolar profiles and calculated their surface as if they were circular. In the case of AVi, the outer space was excluded.

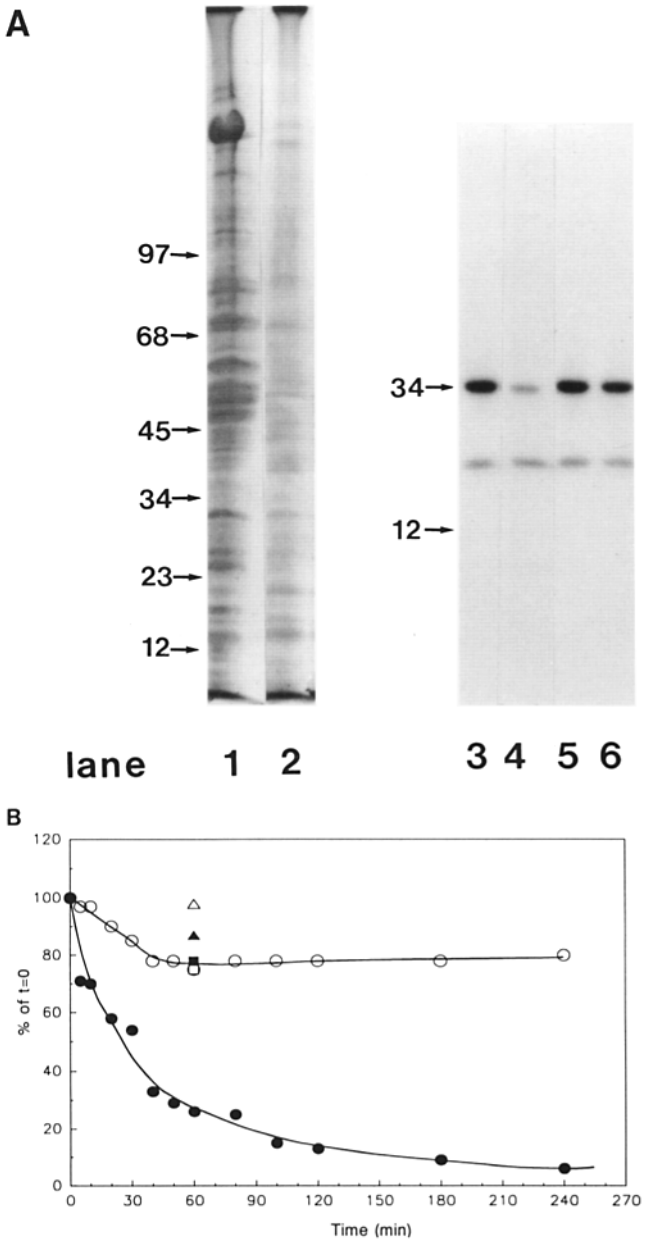

Figure 2. In vitro degradation of CAIII and SOD by lysosomal fractions. (*A*) Incubation of 1:1 mixture of p2 (crude lysosomal fraction) and sup2 (cytosolic fraction) was performed under different conditions (see below and Materials and Methods). After incubation, 10-μl aliquots (corresponding to 76 μg protein, measured before the reaction) were loaded onto either 7–15% (lanes *1* and *2*) or 13% (lane *3–6*) polyacrylamide gels and electrophoresed. Coomassie blue staining of the protein content at time 0 (lane *1*) and after 60 min (lane *2*) shows a general fading of the banding pattern upon incubation at pH 4.5. In immunoblots using mixed antisera (lane *3–6*), SOD (*lower band*) and CAIII (*upper band*) are visualized at time 0 (lane *3*) and after 60 min of incubation at pH 4.5 (lane *4*) or pH 8 (lane 5), or at pH 4.5 in the presence of leupeptin (lane *6*). The migration of molecular mass standards (in kD) is indicated by the arrows. (*B*) The incubation of p2 and sup2 was performed as in *A*, for various times ranging from 0 to 240 min. 10-μl aliquots (corresponding to 76 μg of protein) were analyzed after electrophoresis in a 13% polyacrylamide gel. Quantitation of the bands for SOD (○) and CAIII (●) in immunoblots were expressed as percentage of the amount of protein present at $t = 0$. Triangles and squares correspond to the quantitation of SOD (△, □) and CAIII (▲, ■) in lanes *5* and *6* of Fig. 2 *A*, respectively. The specificity of the two antisera has been tested by incubating two identical blots with only one antibody. We estimated the linearity of the method using pure SOD from liver (Chang et al., 1988; 3 mg/ml) and pure CAIII from skeletal muscle (kindly provided by Dr. K. H. Väänanen; 0.5 mg/ml) as standards in the blotting assay.

Results

Cellular Distribution of CAIII and SOD

Immunolocalization of SOD (Fig. 1 *A*) and CAIII (Fig. 1 *B*) demonstrated that these proteins occur abundantly in the cytosol of parenchymal liver cells of male rats. Both were evenly dispersed throughout the nucleus and cytoplasm, and were not detectable in compartments of the secretory pathway, in mitochondria, or in peroxisomes. However, SOD was found within lysosomes with a labeling density (LD) mostly exceeding that of the cytosol (Fig. 1 *A*). CAIII labeling on the other hand was absent or low in most lysosomal vacuoles except in some vacuoles in which its LD was the same as in cytoplasm (Fig. 1 *B*).

Degradation of CAIII and SOD

To investigate whether differences in sensitivity to lysosomal proteolysis could explain the differential localization of SOD and CAIII in lysosomes, we established an in vitro assay to measure their rate of degradation during incubation with lysosomal enzymes. The assay consisted of a mixture of a crude lysosomal fraction (p2) and a cytosolic fraction (sup2). The starting p2/sup2 mixture showed a complicated protein banding pattern in SDS-PAGE (Fig. 2 *A*, lane *1*). The bands of CAIII and SOD were visualized by immunoblotting: CAIII corresponded to a 34-kD band (Carter et al., 1981) and SOD to a 16-kD band according to the size of its subunits (McCord and Fridovich, 1969; Ho and Crapo, 1987) (Fig. 2 *A*, lane *3–6*). After a 60-min incubation of the p2/sup2 mixture at low pH and in the presence of Triton X-100 at 37°C, protein degradation resulted in a blurred banding pattern in SDS-PAGE (Fig. 2 *A*, lane *2*). Immunoblotting showed that 75% of the CAIII and only 20% of the SOD was degraded (Fig. 2 *A*, lane *4*). This degradation could be inhibited by incubation at pH 8.0 instead of 4.5 (Fig. 2 *A*, lane *5*) or by adding leupeptin to the assay (Fig. 2 *A*, lane *6*). This indicated that SOD was more resistant to lysosomal lytic activity than CAIII.

We followed the time course of in vitro degradation of CAIII and SOD in p2/sup2 mixtures by immunoblotting and densitometry (Fig. 2 *B*). The CAIII level dropped to 6% of its initial value after 4 h of incubation at 37°C showing a half time of 24 ± 2 min while SOD immunoreactivity remained at a constant level during the same time period after an initial drop of ~20%. This initial decrease was also observed in the presence of leupeptin, but not during incubation at pH 8.0 (Fig. 2 *B*). Although these in vitro observations might not reflect the actual degradation rates of CAIII and SOD in vivo, they do suggest that SOD is far more resistant to acid proteolysis than CAIII. It might explain why SOD was predominant in lysosomes, while both were similarly labeled in the cytosol (Fig. 1).

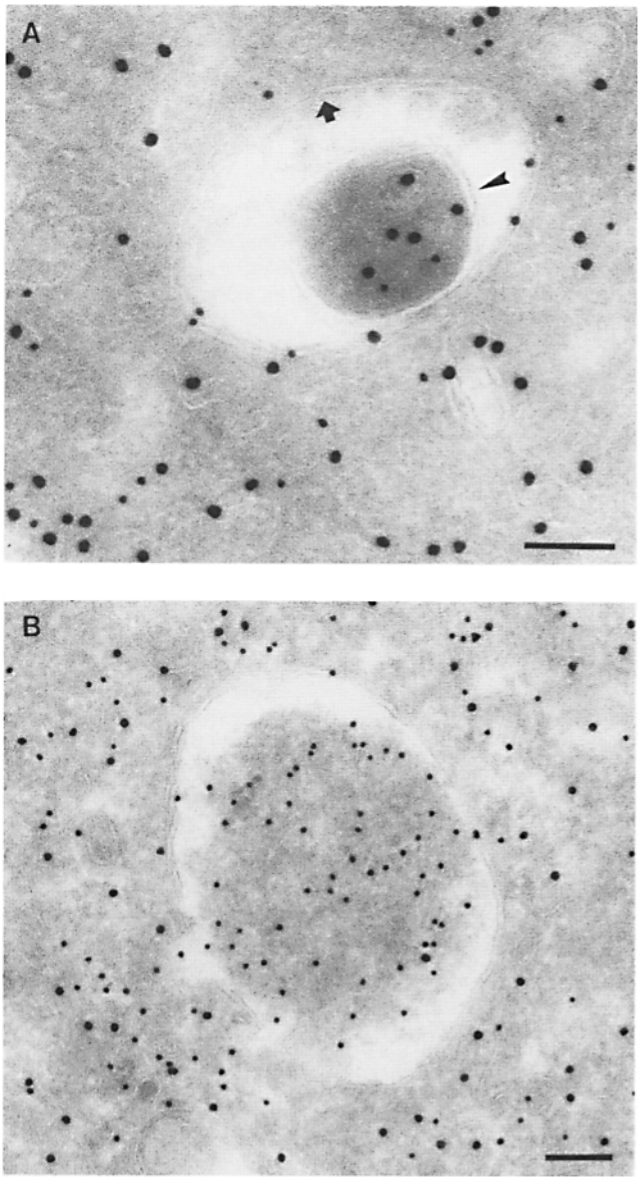

Figure 3. Characteristics of AVi and AVd. Cryosections of fasted rat liver double immunolabeled for CAIII (15-nm gold) and SOD (10-nm gold). (*A*) AVi with a peripheral space between the external (*arrow*) and internal (*arrowhead*) membranes and an internal compartment in which the labeling densities for SOD and CAIII are close to these in the cytoplasm. (*B*) AVd showing a high labeling for SOD and no labeling for CAIII. Bars, 100 nm.

Table I. Relative Frequency and Classes of Autophagic Vacuoles in Liver Parenchymal Cells

	Liver		Hepatocytes	
	Fed	Fasted	+3-MA	−3-MA
AVi	2%	15%		65%
AVd	98%	85%	100%	35%
Total/cell	3 ± 0.5	12 ± 3	1.5 ± 0.5	17 ± 4
Profile	(n = 2)	(n = 3)	(n = 4)	(n = 2)

Livers and hepatocytes were double immunolabeled for CAIII and SOD. Autophagic vacuoles were counted in each cell profile in which the nucleus was cut and classified according to their SOD/CAIII which was ⩽1 for AVi (similar to cytosol) and >1 for AVd. Hepatocytes were cultured for 60 min under autophagy stimulating conditions (see Materials and Methods) with or without the autophagy inhibitor 3-MA. Two experiments have been performed and 50 cells were observed for each condition.

CAIII and SOD in the Autophagic Route

Taking advantage of the differential degradation rate of the SOD and CAIII, we traced the process of autophagy by examining the labeling characteristics for both enzymes in autophagic vacuoles (AV). Cryosections of fasted rat liver were immunogold labeled for both proteins. The labeling ratio of SOD over CAIII (SOD/CAIII) as well as the LD for SOD and CAIII within AV, as compared with that in the cytoplasm, were taken to reflect their autophagic developmental state. Essentially two classes of vacuoles containing SOD and CAIII were encountered. The first class showed a SOD/CAIII ⩽1. The LD for both enzymes was close to that observed in the surrounding cytoplasm. These vacuoles were further characterized by a peripheral space, which was bordered by a membrane at the inner and one at outer side (Fig. 3 *A*), although these were not always visible in the cryosections (Fig. 6). The labeling characteristics are consistent with the idea that these vacuoles are derived from random sequestration of cytoplasm (Dunn, 1990*a*). Accordingly, we designated this class of AV as the initial autophagic vacuoles (AVi) equivalent to autophagosomes described by Marzella and Glaumann (1987), Pfeifer (1987), and Seglen (1987). The space between the outer and inner membrane was artifactually wide in cryosections. It was mostly devoid of electron-dense material and was not labeled for SOD and CAIII (Fig. 3 *A*).

In the second class of vacuoles SOD/CAIII was >1 (Fig. 3 *B*). The LD for SOD in these AV was equal to or higher than in cytoplasm. The CAIII labeling was partly or totally absent, reflecting the apparent lytic activity in these vacuoles (Fig. 3 *B*). Therefore they were called degradative autophagic vacuoles (AVd) (Dunn, 1990*b*). AVd are probably equivalent to autophagolysosomes described by Marzella and Glaumann (1987), Pfeifer (1987), and Seglen (1987). They had a single limiting membrane. The autophagic nature of AVi and AVd was further apparent from the fact that their presence coincided with high levels of autophagy in liver cells (Table I). Such high levels can be induced in liver by fasting (Mortimore, 1987) or in cultured hepatocytes by conditions like amino acid deprivation. Under these conditions we found at least five times more AV of both types than in fed animal tissues or cells incubated under autophagy blocking conditions.

AVi Are Closed Structures

The LD for SOD and CAIII in AVi and cytosol were very similar. Therefore one could argue that AVi profiles may represent structures which are in open contact with the cytoplasm (Fig. 4 *A*) outside the plane of the section. In isolated hepatocytes cultured for 60 min under high autophagy conditions, an average of 15 AV per cell profile were observed. Of these, 65% were AVi (Table I). We used this system to test whether AVi are indeed sealed vacuoles according to two different approaches. First, we mildly disrupted cells by me-

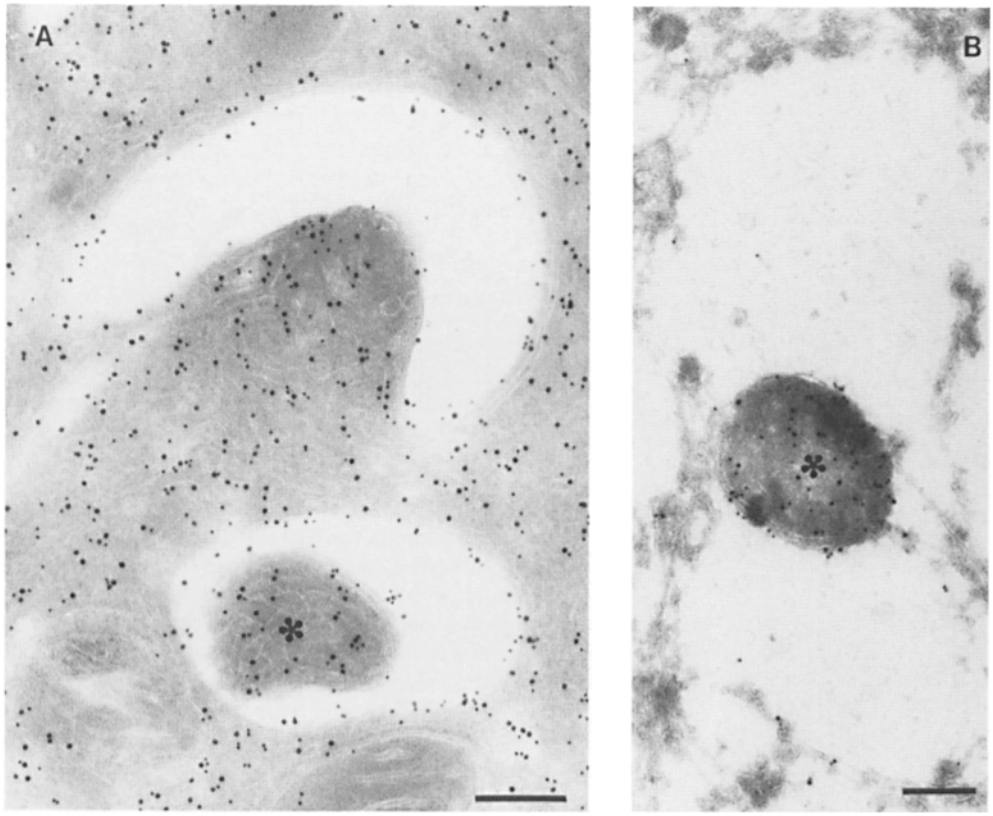

Figure 4. AVi are closed profiles. Hepatocytes incubated for 60 min were fixed in 2% glutaraldehyde (*A*) or were first mildly broken by mechanical force on ice, and then fixed in 2% glutaraldehyde (*B*). LD for SOD (10-nm gold) and CAIII (15-nm gold) are similar in AVi (*asterisks*) and in cytoplasm of intact cells (*A*). The upper profile probably represents a forming AVi with the sequestered material still in open contact with the cytoplasm. In the broken cell (*B*) only a little SOD and CAIII labeling is left in the cytoplasm, whereas the AVi (*asterisks*) had not lost SOD and CAIII reactivity showing that this AVi is sealed. Bars, 200 nm.

A

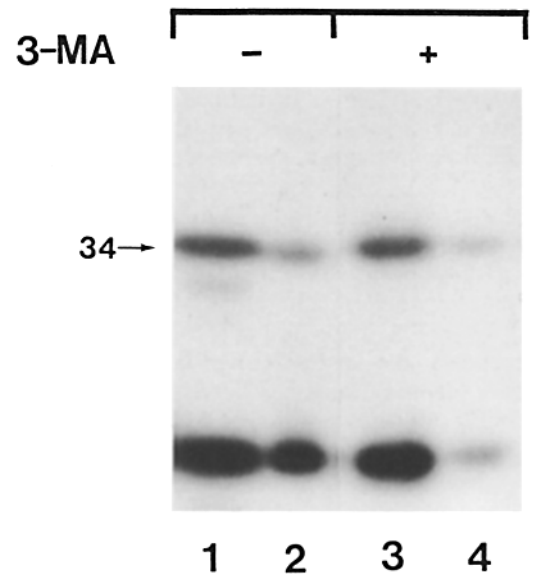

B

Conditions of incubation	60 min	
	−3-MA	+3-MA
% of cytosolic CaIII found in membrane fraction	3.2 ± 0.5 (*n* = 4)	0.9 ± 0.2 (*n* = 2)
% of cytosolic SOD found in membrane fraction	6.3 ± 1 (*n* = 4)	1.1 ± 0.2 (*n* = 2)

chanical force on ice before fixation. This treatment of course affected the morphology of both the cytosol and the AV seriously, but it was quite obvious that the LD of SOD and CAIII in the cytosol decreased strongly because of apparent leakage from the cells, while in most AVi the SOD and CAIII concentration appeared unaffected (Fig. 4 *B*). Since the LD for SOD and CAIII in AVi still reflected LD in cytoplasm of intact cells (Fig. 4 *A*), this demonstrated that the material contained in the vacuoles had not leaked out but was separated from the surrounding cytoplasm.

Figure 5. Effect of 3-MA on the sequestration of cytosolic SOD and CAIII in a membrane fraction. Hepatocytes were isolated and incubated for 60 min under autophagy inducing conditions (removal of amino acids and addition of 1 nM glucagon) in the presence or the absence of 3-MA. The PNS was prepared as described in Materials and Methods and the fractionation was performed by centrifugation through 0.5 M sucrose layered over 0.3 ml and 2 M sucrose for 1 h at 100,000 *g*. The membrane fraction was collected at the interphase between 0.5 M sucrose and 2 M sucrose. Aliquots of PNS and membrane fraction, containing 1/600 and 1/53 of the total fractions, respectively, were loaded in a 13% polyacrylamide electrophoresis gel, and SOD and CAIII were detected as described in the legend of Fig. 2. (*A*) Double immunoblot of SOD (*lower band*) and CAIII (*upper band*) content in PNS (lanes *1* and *3*) and membrane fraction (lanes *2* and *4*) of the hepatocytes incubated 60 min without 3-MA (lanes *1* and *2*) or in the presence of 3-MA (lanes *3* and *4*). (*B*) Quantitation by scanning of the bands corresponding to SOD and CAIII pelleted with the membrane fraction of hepatocytes incubated with or without 3-MA for 60 min. The figures are the percentage of the cytoplasmic SOD and CAIII pelleted with the membrane fraction in each condition.

Table II. Reactivity of AV for Lysosomal Markers

	AVi	AVd
	%	
lgp120 positive	50	100
Cathepsin D positive	41	89

Sections of livers from fasted rats were triple immunogold-labeled for SOD, CAIII, and either lgp120 or cathepsin D. Randomly encountered AV were scored for lgp120 or cathepsin D reactivity, and classified as AVi or AVd as indicated in legend of Table I. 165 and 78 AV were counted in lgp120- and cathepsin D-labeled sections, respectively.

In a second approach, fractionation experiments in which a membrane fraction and PNS were analyzed for their content in SOD and CAIII (Fig. 5 *A*) showed that 3% of the cytosolic CAIII and 6% of the cytosolic SOD was pelleted with the membrane fraction (Fig. 5 *B*). The pelleted CAIII must be enclosed in AVi, since AVd do not contain appreciable amounts of CAIII. The percentage of CAIII that could be precipitated was reduced to <1% (background level of experiment) after a 60-min incubation of the hepatocytes with 3-MA, a drug which has been shown to inhibit autophagy by preventing AVi formation (Seglen and Gordon, 1982). Indeed, virtually no AVi and only a few AVd were present (Table I) comparable to the situation of the starting material.

Distribution of Lysosomal Markers

During development of AVi (SOD/CAIII ≤1) into AVd (SOD/CAIII >1), lysosomal constituents including degradative enzymes are introduced into the AV. We investigated the distribution of lysosomal markers in AV of rat liver tissue to define at which stages this occurs. In addition to CAIII and SOD, sections were immunolabeled for the lysosomal membrane glycoprotein lgp120 or cathepsin D. Half of the AVi were labeled for lgp120 or cathepsin D (Table II) with a low but significant density (Fig. 6 *B* and *C*). The other half was unlabeled (Fig. 6 *A*). Labeling for the lysosomal markers was always confined to the peripheral space of the AVi. It was not

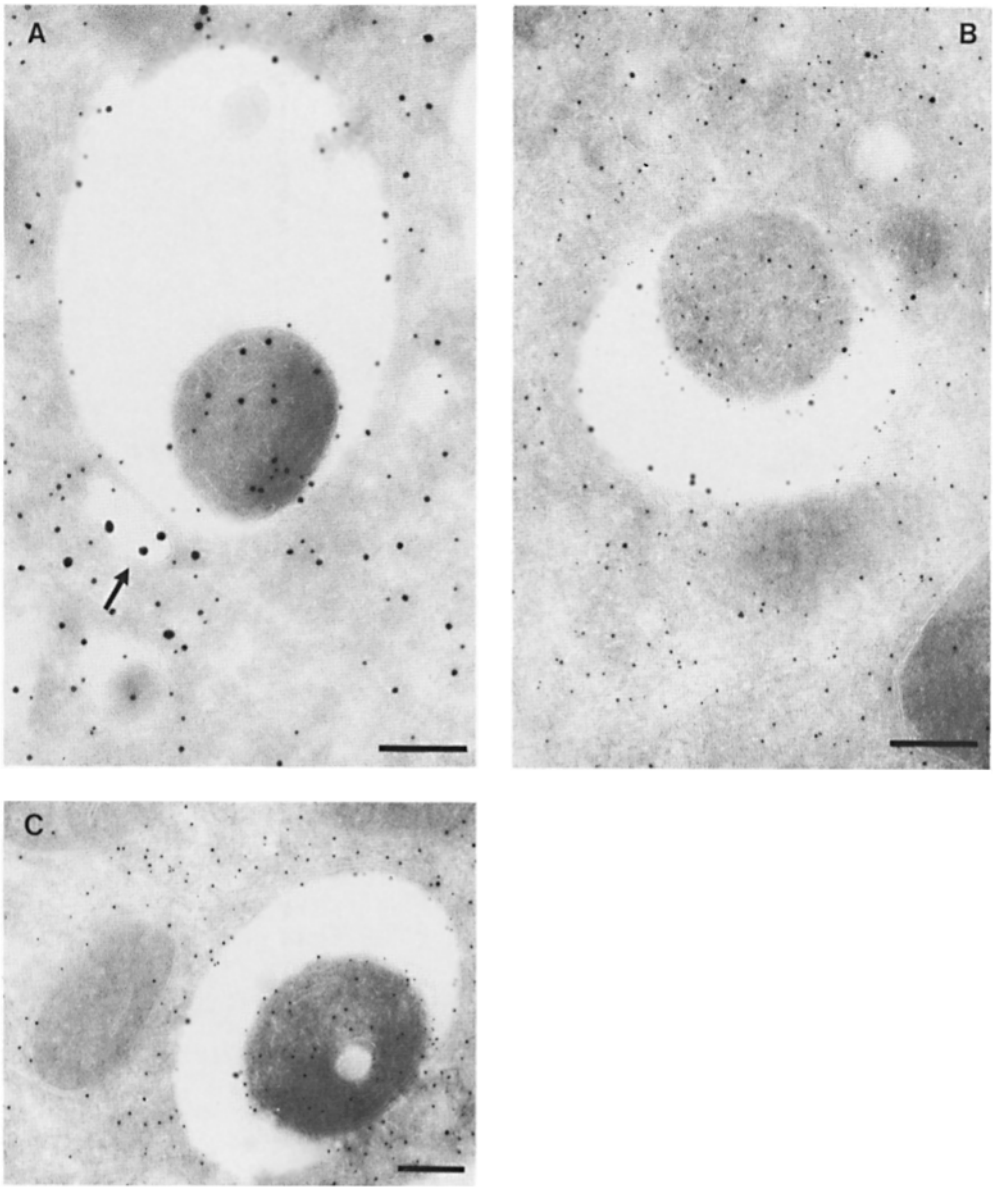

Figure 6. Presence of lysosomal markers lgp120 and cathepsin D in AVi. Triple immunolabeling in *A* is as follows: SOD = 10-nm gold; CAIII = 15-nm gold; and lgp 120 = 20-nm gold; in *B*: SOD = 5-nm gold; CAIII = 10-nm gold; and lgp120 = 15-nm gold; in *C*: SOD = 5-nm gold; CAIII = 10-nm gold; and cathepsin D = 15-nm gold. An AVi nonreactive for lgp120 is shown in *A* with a small lgp120-positive structure in its vicinity (*arrow*). Some labeling for the lysosomal markers is associated with the peripheral space of the AVi in *B* and *C*. The SOD/CAIII of the AVi is similar to the surrounding cytoplasm and lower than 1 in all AVi. Bars, 200 nm.

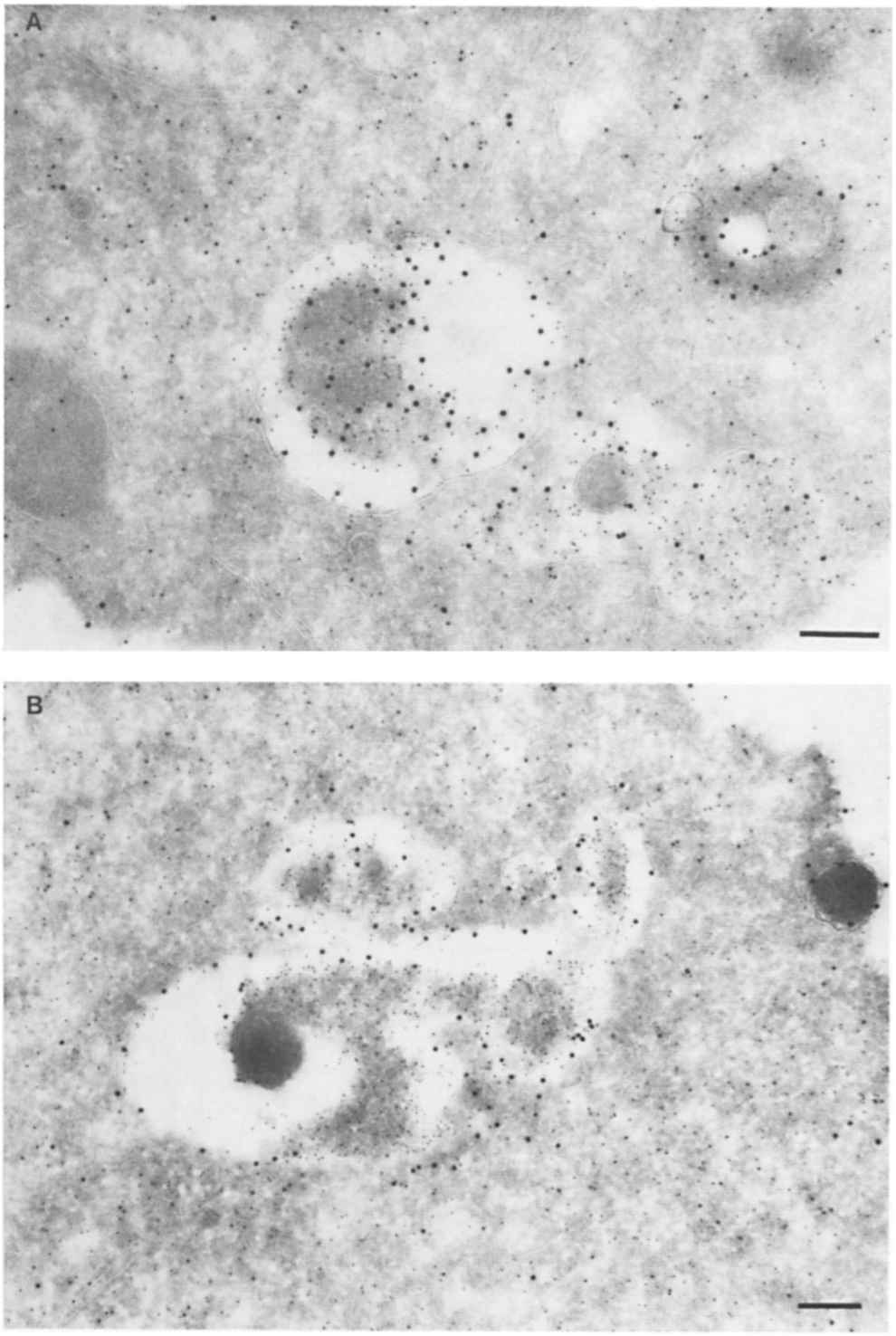

Figure 7. Localization of the lysosomal markers lgp120 and cathepsin D in late AVd. Triple immunolabeling of CAIII (10-nm gold), SOD (5-nm gold), and cathepsin D or/lgp120 (15-nm gold). Cathepsin D (*A*) is located in the content of the AVd, while lgp120 (*B*) is more intense in the AVd membrane. Note the high labeling for SOD and the absence of CAIII in large vacuoles. The AVd are often irregularly shaped, suggesting that they are in process of mutual fusion. Bars, 200 nm.

mixed with the SOD and CAIII-positive material in the core. This observation suggests that these lgp120 and cathepsin D–positive AVi had acquired lysosomal components, but that degradation had not yet started. They therefore were considered as intermediates between AVi and AVd, and are further referred to as AVi/d in accordance with previously introduced nomenclature (Dunn, 1990*b*). Sometimes small structures, positive for lgp120 (Fig. 6 *A*) and for cathepsin D (not shown), were observed in the vicinity of AVi.

On the other hand, the vast majority of AVd was labeled for lgp120 and cathepsin D (Table II) in agreement to their degradative activity (degradation of CAIII). Labeling for cathepsin D was fairly strong throughout the content (Fig. 7 *A*) while lgp120 labeling was mainly associated with the limiting membrane (Fig. 7 *B*). Some AVd profiles suggested that these vacuoles contained a subcompartment with a SOD/ CAIII similar to cytoplasm and AVi (Fig. 8 *B*). The membrane around this subcompartment was strongly labeled for lgp120 and its content was negative for cathepsin D (Fig. 8 *A*). We propose that such subcompartments derive from

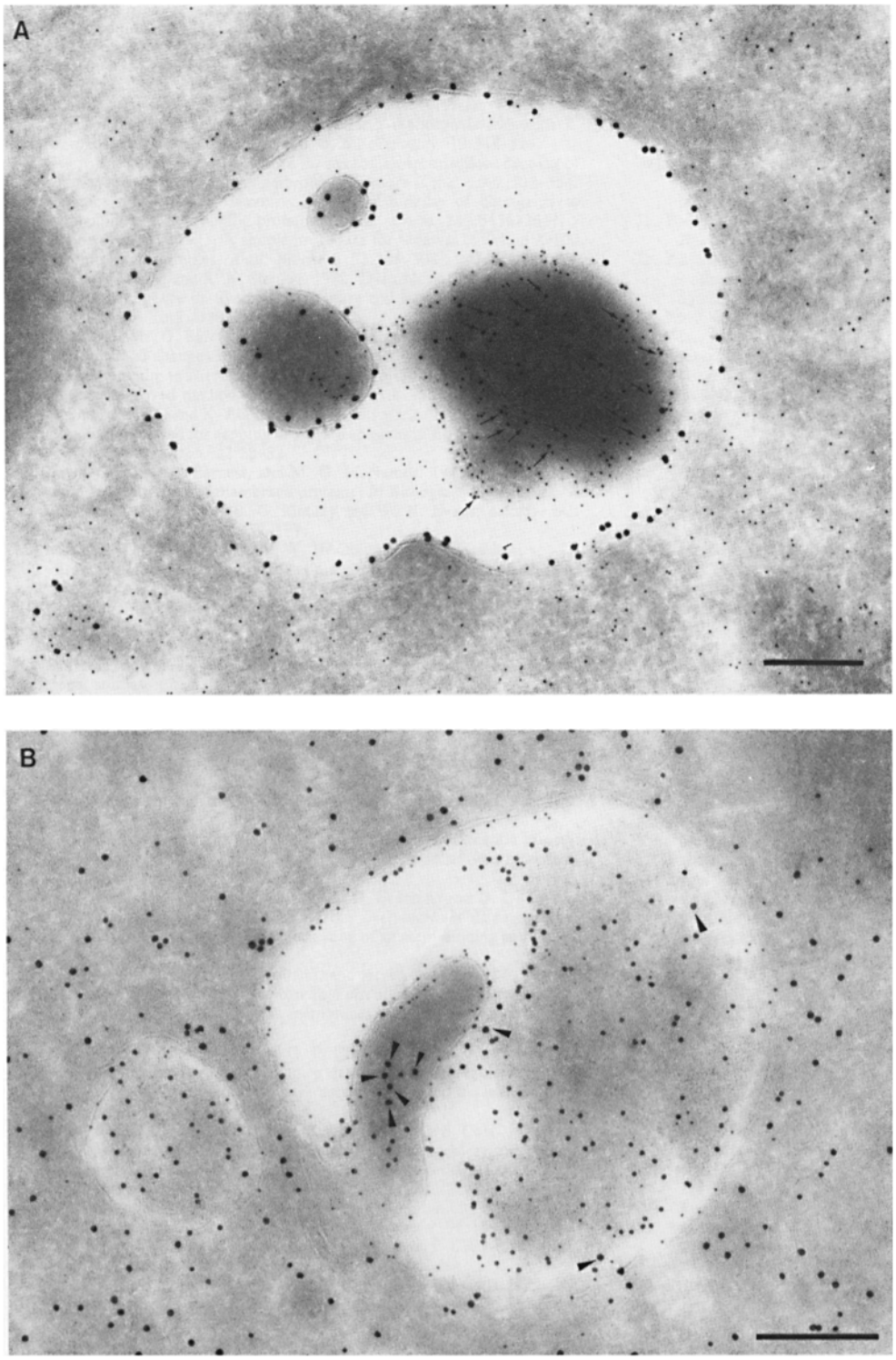

Figure 8. Localization of the lysosomal markers lgp120 and cathepsin D in late AVd. The membrane of the AVd is highly reactive for lgp120 (15-nm gold in *A* and 5-nm gold in *B*), as are the two inclusions present at the left side of the vacuoles. Cathepsin D (10-nm gold in *A*, *arrows*) is mixed with the degrading material at the right side, where also SOD (5-nm gold in *A* and 10 nm in *B*) is accumulated, while barely any CAIII (15-nm gold in *B*) is present. The inclusions have a LD for SOD (5-nm gold in *A* and 10-nm gold in *B*) and for CAIII (15-nm gold in *B*, *arrowheads*) similar to those in the cytoplasm. Bar, 200 nm.

secondary invaginations of the outer membrane of AVd. This activity of autophagic vacuoles has been described before as microautophagy (Marzella and Glaumann, 1987) or as lysosomal wrapping (Sakai et al., 1989).

The Degradative Autophagic Vacuoles

The AVd were very heterogeneous. Apart from a decrease in LD for CAIII, many of the AVd showed a high SOD/CAIII due to a considerable increase in their LD for SOD as compared with that in the cytoplasm (concentration factor for SOD). The size of the AVd also varied strongly. We analyzed the concentration factor for SOD and the surface area of randomly selected AV profiles in the sections. These data were plotted versus their SOD/CAIII (Fig. 9). The vacuoles with a SOD/CAIII ≤ 1 represented the AVi, including the AVi/d, and exhibited a LD for SOD close to that in the cytoplasm (concentration factor for SOD ≈ 1). Their size was relatively uniform with an average surface area of 1.5 μm^2. The AVd,

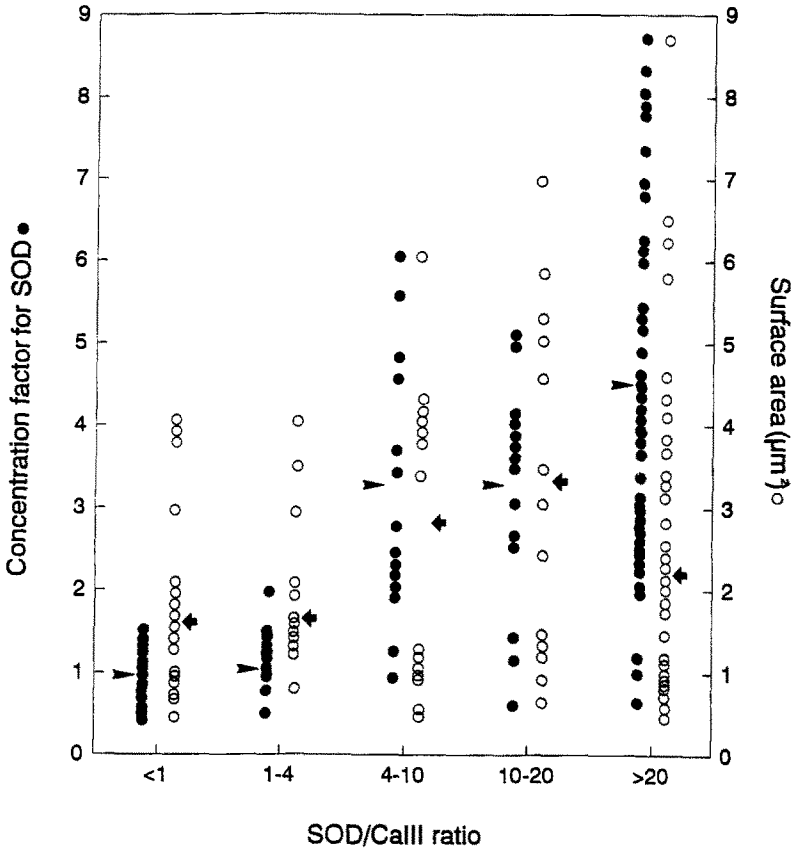

Figure 9. AV were classified in five groups according to their SOD/CAIII and the concentration factor for SOD (•, left scale) and the surface area (○, right scale) are plotted for each of them. Average values within each group are indicated by arrowheads and arrows, respectively.

i.e., vacuoles with SOD/CAIII >1, could be divided into two subclasses according to their size and LD for SOD. The first one with SOD/CAIII between 1 and 4 (Fig. 9) showed a concentration factor for SOD of ~1 and an average size of 1.7 μm^2. These AVd only differed from AVi by showing a lower CAIII labeling and by their lack of a typical peripheral space. We tentatively call them early AVd deriving from AVi/d shortly after dissolution of the inner membrane allowing lytic enzymes from the peripheral space to reach and degrade the autophagocytosed material (lower CAIII labeling). The second subclass, represented by the three groups with SOD/CAIII >4 (Fig. 9) presented a high concentration factor for SOD and a higher variance in size whose average values clearly exceeded that of AVi and early AVd. This second subclass, called late AVd, could derive from the fusion of preexisting AVd and newly formed early AVd. Repeated fusion (resulting in irregular profiles, Fig. 7 *B*) and membrane retrieval (wrapping, Fig. 8) seemed to take place extensively among these late AVd, resulting in accumulation of degradation-resistant materials.

Discussion

CAIII and SOD are abundant cytosolic proteins in male rat liver cells. In addition, SOD but not CAIII is present in lysosomal structures. This is due to the high resistance of SOD to lysosomal proteolysis while CAIII is rapidly degraded under the same conditions. The presence of SOD in lysosomes is probably the result of autophagy since it coincides with the onset of autophagy. The aim of this study was to describe the autophagic pathway in liver by using CAIII and SOD as endogenous markers. We double immunogold-labeled cryosections of liver and of isolated hepatocytes for the localization of SOD and CAIII. The labeling ratio of SOD over CAIII was calculated to classify autophagic vacuoles according to different stages of autophagy on the basis of the differential degradation rates of the two proteins. Furthermore, the distribution of the lysosomal markers lgp120 and cathepsin D in the autophagic compartments was studied to define at which stage lysosomal components are introduced into the autophagic route. The observations suggest three sequential autophagic events (Fig. 10).

The Appearance of AVi

SOD as well as CAIII are evenly distributed throughout the cytoplasm. The initial random sequestration of pieces of cytoplasm leads to the formation of AVi, with SOD and CAIII labeling characteristics similar to the cytosol. AVi were observed in fasted but not in fed rat liver and were present in isolated hepatocytes incubated in the absence of amino acids to induce autophagy, but were absent when the cells were incubated in the presence of 3-MA to block the first sequestration process of autophagy (Seglen and Gordon, 1982). AVi showed two limiting membranes, in agreement with the idea that a cisternal element is engaged in the first engulfment of cytoplasm (Marzella and Glaumann, 1987; Dunn, 1990*a*; Furuno et al., 1990). Only occasionally AVi were encountered with a nonclosed double-membrane but most of them were sealed. This was shown in two ways. First,

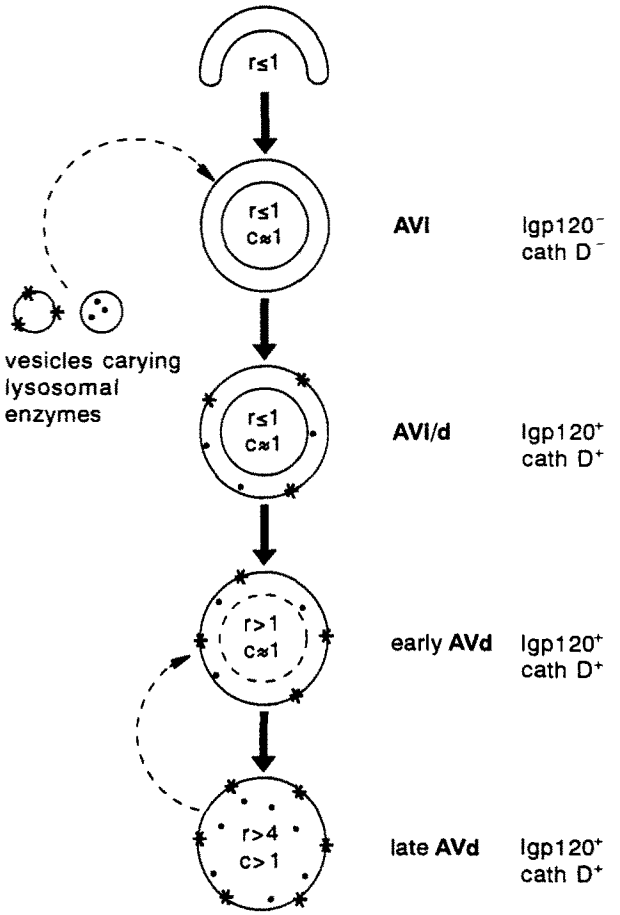

Figure 10. Schematic representation of the proposed steps in autophagy. AVi form upon fasting and have a SOD/CAIII (r) ≤1 and a concentration factor for SOD (c) ≈1. AVi acquire lysosomal components by fusion with small structures containing lysosomal markers (lgp120 [*] and cathepsin D [*dots*]) while the included cytoplasm is still enclosed by an internal membrane. This results in the formation of AVi/d which are intermediate between AVi and AVd. Actual degradation starts as soon as the inner membrane disappears, which results in the decrease of CAIII labeling in early AVd ($1 < r < 4$, and $c \approx 1$). During maturation into late AVd ($r > 4$; $c > 1$), a complicated remodeling of the vacuoles by mutual fusion and wrapping results in changes in the vacuolar size and concentration of compounds which are resistant to degradation like SOD. The fusion events are represented in dashed arrows and maturation events in bold arrows.

the labeling densities of SOD and CAIII in AVi were not affected by damaging the cells which dramatically decreased the cytosolic labeling. Second, by cell fractionation we show that 3.2% of CAIII is pelletable together with membranes, a feature that was reduced to <1% after blocking of AVi formation with 3-MA. Since the morphology showed that almost all sequestered CAIII is present in AVi, together these data show that the majority of AVi are closed structures.

Maturation of AVi into Early AVd

Before the stage of AVd, lysosomal constituents must be delivered to the vacuoles. This may occur by fusion of AVi with either preexisting AVd (lysosomes) (Mortimore, 1987; Marzella and Glaumann, 1987) or with nonautophagic structures containing lysosomal components such as *trans*-Golgi reticulum-derived carrier vesicles and/or late endosomes (Tooze et al., 1990). Two arguments favor the possibility of fusion with small nonautophagic structures. The first is that the absence of SOD in the peripheral space of AVi/d would not have been the case after fusion with preexisting, late AVd. Secondly, we did not find a significant increase in size of the AV before the late AVd stage. Together these observations suggest that the first step in the maturation of AVi, i.e., the formation of AVi/d, is fusion with small SOD-negative, and lgp120-and/or cathepsin D–positive structures such as we observed sometimes in the immediate environment of AVi. The nature of the structures has to be evaluated. The existence of AVi/d has also been reported by Dunn (1990*a*) and Furuno et al. (1990) who showed that the outer membrane of some AV contained patches of lysosomal components.

Maturation of Early AVd into Late AVd

Early AVd probably develop into late AVd by fusion with each other and with preexisting late AVd. This would explain why AVd vary in SOD LD and size so widely (Fig. 9). The involvement of lysosome fusion with early autophagic stages as a step in AV maturation has been described before (Marzella and Glaumann, 1987; Pfeifer, 1987). Our observations indicated that such fusion events were restricted mainly to different stages of AVd, while AVi seemed far less involved (see also above). The presence of inclusions with cytosolic characteristics in AVd suggests that AVd are also capable of secondary engulfment of parts of cytoplasm. Such a lysosomal wrapping (Marzella and Glaumann, 1987; Sakai et al., 1989) might be an integral process of autophagy by which the vacuolar growth due to fusions is counteracted.

The resistance of SOD against lysosomal degradation makes this protein a useful tool for measuring the capacity of autophagy in cells. This is apparent from the fact that 6.3% of the SOD is found in the lysosomal fraction after 1 h of autophagy (and only 1% after treatment with 3-MA), which corresponds fairly well with the hourly total autophagic protein degradation of 4–6% reported for cultured cells (Seglen, 1987).

We have found that all lysosomes (lgp120- and cathepsin D–positive) contained SOD. Thus, under steady-state autophagic conditions, all hepatic lysosomes seem to participate in degradation of cytoplasmic material. This suggests that the autophagic process contributes to the biogenesis of lysosomes as does endocytosis and the phagocytic route. Where in hepatocytes endocytosed material meets autophagocytosed SOD and CAIII is currently under study.

The authors would like to thank Dr. Matt Geelen for providing isolated hepatocytes; Dr. Kalervo Väänänen for providing the CAIII antibodies; Tom van Rijn, Maurits Niekerk, and Rene Scriwanek for excellent photographic work; and Dr. Willem Stoorvogel and Adrian Oprins for their stimulating discussions.

This work was supported in part by National Heart, Lung, and Blood Institute grant PO1 HI 31992 and RO1 HL 42609 to J. D. Crapo and by NWO Nederlandse organisatie voor Wetensdrappelijk Onderzoek program, grant 900-523-094.

Received for publication 6 April 1992 and in revised form 2 November 1992.

References

Beynen, A. C., and M. J. H. Geelen. 1984. Relation between fatty acid synthesis, pyruvate concentration and cell concentration of suspensions of isolated rat hepatocytes. *Int. J. Biochem.* 16:105–107.

Beynen, A. C., W. J. Vaartjes, and M. J. H. Geelen. 1979. Opposite effect of insulin and glucagon in acute hormonal control of lipogenesis. *Diabetes.* 28:828–835.

Bradford, M. M. 1976. A rapid and sensitive method for the quantitation of microgram quantities of protein utilizing the principles of protein-dye binding. *Anal. Biochem.* 72:248–254.

Carter, N. D., D. Hewett-Emmett, S. Jeffrey, and R. E. Tashian. 1981. Testosterone-induced, sulfamide-resistant carbonic anhydrase isoenzyme of rat liver is indistinguishable from skeletal muscle carbonic anhydrase III. *FEBS (Fed. Eur. Biochem. Soc.) Lett.* 128:114–118.

Chang, L. Y., J. W. Slot, H. J. Geuze, and J. D. Crapo. 1988. Molecular immunocytochemistry of the CuZn superoxide dismutase in rat hepatocytes. *J. Cell Biol.* 107:2169–2179.

Chiang, H. L., and J. F. Dice. 1986. Peptides sequences that target proteins for enhanced degradation during serum withdrawal. *J. Biol. Chem.* 263: 6797–6805.

Chiang, H. L., S. R. Terlecky, C. P. Plant, and J. F. Dice. 1989. A role for a 70-kilodalton heat shock protein in lysosomal degradation of intracellular proteins. *Science (Wash. DC.).* 242:382–385.

De Duve, C., B. C. Pressman, R. Gianetto, R. Wattiaux, and F. Appelmans. 1955. Tissue fractionation studies. 6. Intracellular distribution pattern of enzymes in rat-liver tissue. *Biochem. J.* 60:604–617.

Dunn, W. A. 1990*a*. Studies on the mechanisms of autophagy: formation of the autophagic vacuole. *J. Cell Biol.* 110:1923–1933.

Dunn, W. A. 1990*b*. Studies on the mechanisms of autophagy: maturation of the autophagic vacuole. *J. Cell Biol.* 110:1935–1945.

Furuno, K., T. Ishikawa, K. Akasaki, S. Lee, Y. Nishimura, H. Tsuji, M. Himeno, and K. Kato. 1990. Immunocytochemical study of the surrounding envelope of autophagic vacuoles in cultured rat hepatocytes. *Exp. Cell Res.* 189:261–268.

Geuze, H. J., J. W. Slot, P. A. van der Ley, R. C. T. Scheffer, and J. M. Griffith. 1981. Use of colloidal gold particles in double-labeling immunoelectron microscopy of ultrathin frozen tissue sections. *J. Cell Biol.* 89: 653–665.

Geuze, H. J., J. W. Slot, G. J. Strous, A. Hasilik, and K. Von Figura. 1985. Possible pathways for lysosomal enzymes delivery. *J. Cell Biol.* 101:2253–2262.

Geuze, H. J., W. Stoorvogel, G. J. Strous, J. W. Slot, J. E. Bleekemolen, and I. Mellman. 1988. Sorting of mannose 6-phosphate receptors and lysosomal membrane proteins in endocytic vesicles. *J. Cell Biol.* 107:2491–2501.

Gordon, P. B., and P. O. Seglen. 1988. Prelysosomal convergence of autophagic and endocytic pathways. *Biochem. Biophys. Res. Commun.* 151: 40–47.

Gruenberg, J., and K. E. Howell. 1989. Membrane traffic in endocytosis: insight from cell-free assays. *Annu. Rev. Cell Biol.* 5:453–481.

Ho, Y. S., and J. D. Crapo. 1987. cDNA and deduced amino acid sequence of rat copper zinc containing superoxide dismutase. *Nucleic Acids Res.* 15:6746.

Kopitz, J., G. O. Kisen, P. B. Gordon, P. Bohley, and P. O. Seglen. 1990. Nonselective autophagy of cytosolic enzymes in isolated rat hepatocytes. *J. Cell Biol.* 111:941–953.

Kornfeld, S., and I. Mellman. 1989. The biogenesis of lysosomes. *Annu. Rev. Cell Biol.* 5:483–525.

Laemmli, U. K. 1970. Cleavage of structural proteins during the assembly of the head of bacteriophage T4. *Nature (Lond.).* 227:680–685.

Laurila, A. L., E. K. Parvinen, J. W. Slot, and H. K. Väänanen. 1989. Consecutive expression of carbonic anhydrase isoenzymes during development of rat liver and skeletal muscle differentiation. *J. Histochem. Cytochem.* 37:1375–1382.

Marzella, L., and H. Glaumann. 1987. Autophagy, microautophagy and crinophagy as mechanisms for protein degradation. *In* Lysosomes: Their Role in Protein Degradation. H. Glaumann and J. Ballard, editors. Academic Press Inc., Orlando, FL. 319–370.

McCord, J. M., and I. Fridovich. 1969. Superoxide dismutase. An enzymic function for erythrocuprein. *J. Biol. Chem.* 244:6049–6055.

Mortimore, G. E. 1987. Mechanism and regulation of induced and basal protein degradation in the liver. *In* Lysosomes: Their Role in Protein Degradation. H. Glaumann and J. Ballard, editors. Academic Press Inc., Orlando, FL. 415–444.

Peters, P. J., J. Borst, V. Oorschot, M. Fukuda, O. Krahenbuhl, J. W. Slot, and H. J. Geuze. 1991. Cytotoxic T lymphocyte granules are secretory lysosomes, containing both perforin and granzymes. *J. Exp. Med.* 173:1099–1109.

Pfeifer, U. 1987. Functional morphology of the lysosomal apparatus. *In* Lysosomes: Their Role in Protein Degradation. H. Glaumann and J. Ballard, editors. Academic Press Inc., Orlando, FL. 3–59.

Rijnboutt, S., H. M. J. Aerts, H. J. Geuze, J. M. Tager, and G. J. Strous. 1991. Mannose-6-phosphate independent membrane association of cathespin D, glucocerebrosidase and sphingolipid-activating proteins in HepG2 cells. *J. Biol. Chem.* 266:4862–4868.

Sakai, M., N. Araki, and K. Ogawa. 1989. Lysosomal movements during heterophagy and autophagy with special references to nematolysosomes and wrapping lysosomes. *J. Electron. Microsc. Techn.* 12:101–131.

Schworer, C. M., and G. E. Mortimore. 1979. Glucagon-induced autophagy and proteolysis in rat liver: mediation by selective deprivation of intracellular amino acids. *Proc. Natl. Acad. Sci. USA.* 76:3169–3173.

Seglen, P. O. 1987. Regulation of autophagic protein degradation in isolated liver cells. *In* Lysosomes: Their Role in Protein Degradation. H. Glaumann and J. Ballard, editors. Academic Press Inc., Orlando, FL. 371–414.

Seglen, P. O., and P. Bohley. 1991. Autophagy and other vacuolar protein degradation mechanisms. *Experientia (Basel).* 48:158–172.

Seglen, P. O., and P. B. Gordon. 1982. 3-Methyladenine: specific inhibitor of autophagic/lysosomal protein degradation in isolated rat hepatocytes. *Proc. Natl. Acad. Sci. USA.* 79:1889–1892.

Slot, J. W., H. J. Geuze, B. A. Freeman, and J. D. Crapo. 1986. Intracellular localization of the copper zinc and manganese superoxide dismutase in rat liver parenchymal cells. *Lab Invest.* 55:363–369.

Slot, J. W., H. J. Geuze, and A. H. Weerkamp. 1988. Localisation of macromolecular components by application of the immunogold technique on cryosectioned bacteria. *Methods Microbiol.* 20:211–236.

Slot, J. W., H. J. Geuze, S. Gigengack, G. E. Lienhard, and D. E. James. 1991. Immuno-localization of the insulin regulatable glucose transporter in brown adipose tissue of the rat. *J. Cell Biol.* 113:123–135.

Tokuyasu, K. T. 1980. Immunocytochemistry on ultrathin sections. *Histochem. J.* 12:381–403.

Tooze, J., M. Hollinshead, T. Ludwig, K. Howell, B. Hoflack, and H. Kern. 1990. In exocrine pancreas, the basolateral endocytic pathway converges with the autophagic pathway immediately after the early endosome. *J. Cell Biol.* 111:329–345.